

RESEARCH ARTICLE | APRIL 10 2024

## Analysis of the role of the ion polarization current on the onset of pre-disruptive magnetic islands in JET

Special Collection: [1st European Conference on Magnetic Reconnection in Plasmas](#)

L. Bonalumi ; E. Alessi ; E. Lazzaro ; S. Nowak; C. Sozzi ; D. Frigione; L. Garzotti ; E. Lerche ; F. Rimini ; D. Van Eester ; JET Contributors



*Phys. Plasmas* 31, 042505 (2024)

<https://doi.org/10.1063/5.0189722>



### Articles You May Be Interested In

Calculation of toroidal Alfvén eigenmode mode structure in general axisymmetric toroidal geometry

*Phys. Plasmas* (July 2024)

Stabilizing effect of helical current drive on tearing modes

*Phys. Plasmas* (January 2018)

Stabilization of tearing modes by modulated electron cyclotron current drive

*AIP Advances* (January 2019)

25 October 2024 17:42:10



Physics of Plasmas

Special Topics Open  
for Submissions

[Learn More](#)



# Analysis of the role of the ion polarization current on the onset of pre-disruptive magnetic islands in JET

Cite as: Phys. Plasmas **31**, 042505 (2024); doi: 10.1063/5.0189722

Submitted: 30 November 2023 · Accepted: 18 March 2024 ·

Published Online: 10 April 2024



View Online



Export Citation



CrossMark

L. Bonalumi,<sup>1,2,a)</sup> E. Alessi,<sup>2,b)</sup> E. Lazzaro,<sup>2,c)</sup> S. Nowak,<sup>2,d)</sup> C. Sozzi,<sup>2,e)</sup> D. Frigione,<sup>3,f)</sup> L. Garzotti,<sup>4,g)</sup> E. Lerche,<sup>5,h)</sup> F. Rimini,<sup>4,i)</sup> D. Van Eester,<sup>5,j)</sup> and JET Contributors<sup>k)</sup>

## AFFILIATIONS

<sup>1</sup>Physics Department, Università degli Studi Milano Bicocca, Milan 20126, Italy

<sup>2</sup>Istituto Scienza e Tecnologia per il Plasma (ISTP-CNR), Milan 20126, Italy

<sup>3</sup>Università degli Studi di Roma "Tor Vergata", Rome 00133, Italy

<sup>4</sup>UKAEA, Culham Science Centre, Abingdon OX14 3DB, United Kingdom

<sup>5</sup>Laboratory for Plasma Physics, ERM/KMS, Brussels 1000, Belgium

**Note:** This paper is part of the Special Topic on 1st European Conference on Magnetic Reconnection in Plasmas.

<sup>a)</sup> Author to whom correspondence should be addressed: [luca.bonalumi@istp.cnr.it](mailto:luca.bonalumi@istp.cnr.it)

<sup>b)</sup> Electronic mail: [edoardo.alessi@istp.cnr.it](mailto:edoardo.alessi@istp.cnr.it)

<sup>c)</sup> Electronic mail: [enzo.lazzaro@istp.cnr.it](mailto:enzo.lazzaro@istp.cnr.it)

<sup>d)</sup> Electronic mail: [silvana.nowak@istp.cnr.it](mailto:silvana.nowak@istp.cnr.it)

<sup>e)</sup> Electronic mail: [Carlo.sozzi@istp.cnr.it](mailto:Carlo.sozzi@istp.cnr.it)

<sup>f)</sup> Electronic mail: [domenico.frigione@uniroma2.it](mailto:domenico.frigione@uniroma2.it)

<sup>g)</sup> Electronic mail: [Luca.Garzotti@ukaea.uk](mailto:Luca.Garzotti@ukaea.uk)

<sup>h)</sup> Electronic mail: [Ernesto.Lerche@ukaea.uk](mailto:Ernesto.Lerche@ukaea.uk)

<sup>i)</sup> Electronic mail: [Fernanda.rimini@ukaea.uk](mailto:Fernanda.rimini@ukaea.uk)

<sup>j)</sup> Electronic mail: [D.Van.Eester@fz-juelich.de](mailto:D.Van.Eester@fz-juelich.de)

<sup>k)</sup> See the author list of "Overview of JET results for optimizing ITER operation" by J. Mailloux *et al.* Nucl. Fusion **62**, 042026 (2022).

## ABSTRACT

The problem of the trigger of the neoclassical tearing mode is addressed in this work by evaluating the non-linear terms of the generalized Rutherford equation (GRE) for a set of JET disruptions. The linear stability index  $\Delta_0'$ , even for positive values, is not enough to describe the trigger of the mode as the stabilizing non-linear effects tend to prevent the growth of a mode below a certain width. First, an analysis on the contribution of the stabilizing effect of the curvature and the destabilizing effect of the bootstrap is done. Second, the work focuses on the role of the ion polarization current, a return current that flows parallel to the magnetic field due to the difference in the drift motion of the electrons and ions. This contribution is thought to play an important role in the onset of an island of width  $W$ , because it scales as  $1/W^3$ , making it a dominant term in the GRE when  $W$  is small. The assessment is carried out over a subset of pulses, producing interesting observations that were then generalized across the entire database, obtaining consistent results.

© 2024 Author(s). All article content, except where otherwise noted, is licensed under a Creative Commons Attribution (CC BY) license (<https://creativecommons.org/licenses/by/4.0/>). <https://doi.org/10.1063/5.0189722>

## I. INTRODUCTION

The sudden loss of confinement of the plasma, which occurs during disruptions, may result from the onset of a low-mode-number helical magnetic instability, which is eventually responsible for a full collapse of the magnetic equilibrium topology in the plasma. However,

the operation of modern tokamaks has been improved to the point that discharges can proceed unperturbed even in high-performance regimes and instabilities can be avoided by keeping the safety factor  $q$  large enough, up to exhaustion of the inductive flux. Still occasionally without easily identifiable causes (such as impurities influx and

enhanced radiation), an apparently quiescent equilibrium condition, collapses on a short timescale in clear association with footprints of tearing modes onset, both classical and neoclassical (at finite  $\beta_p$ ), occurring at  $q$  rational magnetic surfaces. The fast decrease in the magnetic field can induce strong currents that lead to mechanical stresses on the metallic vessel, which can damage the machine itself. As a consequence, the tokamak operability is usually limited in order to avoid disruptions. Disruptions occur following different sequence of events, whose details depend on the primary cause and, when a plasma control system is active, on the response to such events. The chain of primary causes and subsequent events is an object of active research. Recently, Pucella *et al.*<sup>1</sup> identified disruption paths in JET related to the connection between heavy impurity dynamics and triggering of tearing modes. In particular, they identified two possible paths, connected to the change in the temperature profile. The first one (temperature hollowing) is related to the penetration of impurities, which cools down the plasma core by radiation, producing a hollowing of the temperature profile on the plasma axis. A second path (edge cooling) is connected to a local flattening of the temperature profile at the edge of the plasma caused by a loss of radiated energy associated with impurities. Sozzi *et al.*<sup>2</sup> analyzed a database of JET disruptions, creating a solid statistic that confirms that most pulses follow the two paths previously identified. As highlighted by Vries *et al.*,<sup>3</sup> accidental disruptions are in most cases preceded by the onset, the development, and the locking of a  $2/1$  magnetic island. A deep understanding of the phenomena that lead to a disruption must involve the study of the appearance of a  $2/1$  tearing mode (TM), which, possibly in conditions of overcritical  $\beta_p$ , leads to the trigger of a neoclassical tearing mode (NTM). Pucella *et al.*<sup>1</sup> found out that the change in the temperature due to the hollowing of the temperature or to the edge cooling (EC) leads to a linear destabilization of the  $2/1$  tearing mode. Despite this, the problem related to the trigger of the mode is not clear at all, as the linear stability does not completely determine the behavior of the instability. The non-linear Rutherford's theory<sup>4</sup> predicts the onset of the mode when helical perturbation of the magnetic flux produces a so-called seed island for which the sum of destabilizing effects overcomes the sum of stabilizing effects. Within the different destabilizing effects, the ion polarization current (IOPC) is thought to be particularly crucial in the problem of the onset of the mode.<sup>5,6</sup> A perpendicular current is produced as a result of the island's relative motion with respect to the ions. Then, because of the closure condition  $\nabla \cdot J = 0$ , a parallel current, called ion polarization current, appears, affecting the evolution of the island.<sup>7,8</sup> Following the generalized Rutherford's theory, the contribution of the polarization current can be either stabilizing or destabilizing according to the propagation frequency  $\omega$  of the island in the plasma frame with respect to the electrons and ions diamagnetic frequencies.<sup>9</sup> Furthermore, the effect of the ion polarization current is found in the evolution of an island with width  $W$  scales as  $1/W^3$ . This makes it a key actor able to strongly influence the evolution of an NTM in the initial part of its development. While in the low collisionality conditions, typical of the steady phase of operation, the effect of the ion polarization current is reduced<sup>10</sup> by a factor that scales the inverse aspect ratio  $\varepsilon$  as  $\varepsilon^{3/2}$ , so it is negligible; according to some recent kinetic approaches,<sup>11</sup> destabilizing events such as the EC could induce a decrease in the temperature on the rational surface, increasing the collisionality and the contribution of the ion polarization current, which could become destabilizing. In this work, an analysis on the

non-linear phenomena, which affects the evolution of the magnetic island according to the generalized Rutherford theory, is performed over a database of JET disrupting pulses. In Sec. II A, a description of the model employed is given. In Sec. IV, the results of the analysis are shown. The first part of the analysis is focused on the destabilizing effect of the bootstrap current and on the stabilizing effect of the curvature. Then, the ion polarization current is taken into account for a subset of pulses. Eventually, in Sec. V, the analysis is summarized in order to identify a mechanism able to explain the trigger of the mode and a stability criterion.

## II. PHYSICAL PICTURE

In general, the ion polarization current is a current generated by the differences in the inertial response of the ions and electrons. Here, we provide a physical picture connected to the neoclassical geometry. The intrinsic  $E \times B$  motion of the magnetic island contributes to generate an electric potential, which influences the motion of the particles outside the island.<sup>7,8</sup> Figure 1 represents a cartoon of what the particles experience: in the blue region, the potential due to the island motion generates an  $E \times B$  drift in the opposite direction of the island rotation, while in the green region, the drift velocity points in the same direction. The interaction between the trapped and passing particles in this field generates the neoclassical polarization current. The width of the banana orbit is proportional to the Larmor radius  $\rho_{i,e}$  so that the velocity of a particle lying in the green region during the bouncing back will decrease due to the  $E \times B$  drift, reducing the Larmor radius and then the width of the banana. On average, this corresponds to an outward drift caused by the electric potential generated by the movement of the island. The same, but in the opposite direction, will happen for the particles lying in the blue region. Collision between the trapped and passing particles will generate a current perpendicular to the magnetic island, pointing outward in the green region and inward in the blue

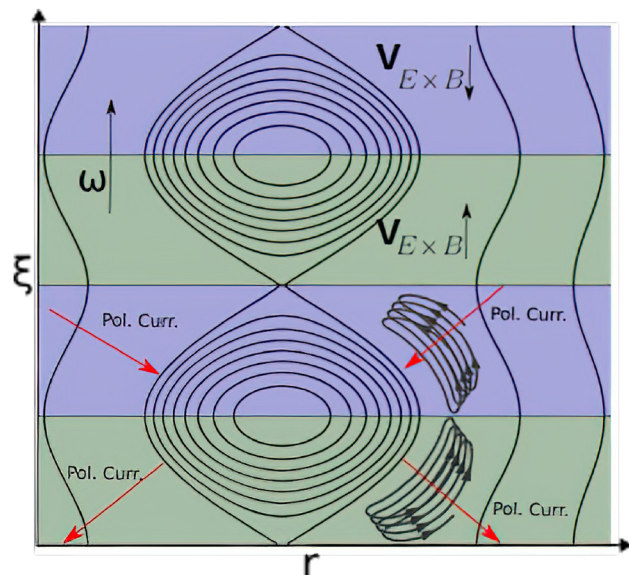


**FIG. 1.** Illustration of the physical picture that leads to the onset of the ion polarization current. The motion of the island generates a potential that affects the neoclassical transport, producing the ion polarization current.

region. This current, called *polarization current*, comes from the movement of trapped particles, proportional to the Larmor radii  $\rho_{i,e}$ . Given that  $\rho_e \ll \rho_i$ , the contribution of electrons is very small, so this current is called *ion polarization current*. A current parallel to the magnetic field is generated in order to preserve the local quasi-neutrality close to the island. This parallel current affects the evolution of the island. According to the physical picture we provided, the strength of the IOPC must depend on the collisionality and rotation frequency of the island in the frame of reference of the plasma. The former contributes to increasing the efficiency with which the trapped particles transfer momentum to passing particles. The latter is proportional to the electric field and the  $v_{E \times B}$  that causes the drift of the trapped particle.

### A. Generalized Rutherford equation

The evolution of the magnetic island is described by the Rutherford theory.<sup>12,13</sup> The non-linear behavior of a magnetic island of width  $W$  is related to the currents parallel to  $B$ . Performing a change of coordinates, from a tokamak frame of reference  $(r(\psi), \theta, \phi)$  to a helical coordinate system  $(x, \xi(\theta, \phi))$  such that

$$\xi = \theta - \phi/q_s, \quad (1)$$

$$x = r - r_s, \quad (2)$$

where  $q$  is the field line winding number. We can integrate the Ampère's law around the island obtaining<sup>11</sup>

$$\frac{g_1 \tau_r}{r_s^2} \frac{dW}{dt} = \Delta'_0 + \int_0^{2\pi} d\xi \int_{-\infty}^{+\infty} J_{\parallel}(\psi) dx. \quad (3)$$

Here,  $g_1$  is a constant,  $\tau_r = \mu_0 r_s^2 / (1.22\eta)$  is the resistive timescale, and  $r_s$  is the position of the rational surface  $q = m/n$  (with  $m, n$  integer). The term  $\Delta'_0$  is the linear stability term, calculated as the logarithmic jump of the perturbed linearized flux  $\tilde{\psi}$  across the rational surface, computed from using the current density profile. The second term on the right-hand side represents the non-linear component of the evolution of the magnetic island. The integral is performed across the rational surface. The function  $J_{\parallel}(\psi)$  can be split into three contributions: the bootstrap current, the Green-Glasser-Johnson (GGJ) term, related to the curvature of the plasma, and the ion polarization current. By computing the integral in Eq. (3) for every contribution to the total  $J_{\parallel}(\psi)$ , we obtain a form of the generalized Rutherford equation as follows:

$$\frac{g_1 \tau_r}{r_s^2} \frac{dW}{dt} = \Delta'_0 + \Delta'_{boot} + \Delta'_{GGJ} + \Delta'_{pol}, \quad (4)$$

$$\Delta'_{boot}(W) = a_{boot} \beta_p \sqrt{\varepsilon} \frac{|L_q|}{|L_p|} \frac{W}{W^2 + W_d^2}, \quad (5)$$

$$\Delta'_{GGJ}(W) = -a_{GGJ} \beta_p \varepsilon^2 \frac{L_q^2}{r_s |L_p|} \left(1 - \frac{1}{q^2}\right) \frac{1}{\sqrt{W^2 + kW_d^2}}, \quad (6)$$

$$\Delta'_{pol}(W) = a_{pol} g(\varepsilon, \nu_{ii}) \beta_p \left(\frac{L_q}{L_p}\right)^2 \frac{\rho_{\theta i}^2 W}{W^4 + W_{\rho}^4} f(\omega), \quad (7)$$

$$f(\omega) = \frac{\omega(\omega - \omega_{*i} - \omega_{*T})}{\omega_{*e}^2}, \quad (8)$$

$$g = \begin{cases} \varepsilon^{3/2} & \nu_{ii}/\varepsilon\omega < \varepsilon^{-3/4} \\ \varepsilon\nu_{ii}^2/\omega^2 & \varepsilon^{-3/4} < \nu_{ii}/\varepsilon\omega < \varepsilon^{-3/2} \\ 1 & \nu_{ii}/\varepsilon\omega > \varepsilon^{-3/2}, \end{cases} \quad (9)$$

where  $\beta_p = 2\mu_0 p^2 / B_0^2$  is the poloidal component of  $\beta$ ,  $\varepsilon$  is the inverse aspect ratio, and  $L_{(*)} = \frac{d^{(*)}}{d^{(*)}/dr}|_{r=r_s}$  is the characteristic length of the pressure  $p$  and the safety factor  $q$  profile. Equation (4) represents the generalized Rutherford equation.<sup>9,13,16</sup> The coefficients  $a_{boot}$ ,  $a_{GGJ}$ , and  $a_{pol}$  are constants, which can be set in order to model the data. In this work, the values of  $a_{boot} = 1.7$  and  $a_{GGJ} = 6$  are chosen following Zohm<sup>17</sup> and Sauter.<sup>18</sup> They also proposed a value for  $a_{pol} \sim O(1)$ ; however, it comprehends the dependence on the rotation frequency. In our model, the rotation frequency is taken into account in the function  $f(\omega)$ , which varies in a wide range ( $f(\omega) = 10 - 200$ ) as shown in Fig. 2. To model suitably the IOPC effect, we choose  $a_{pol} = 0.01$  so that  $a_{pol} f(\omega) \sim O(1)$  is consistent with the results proposed by Zohm

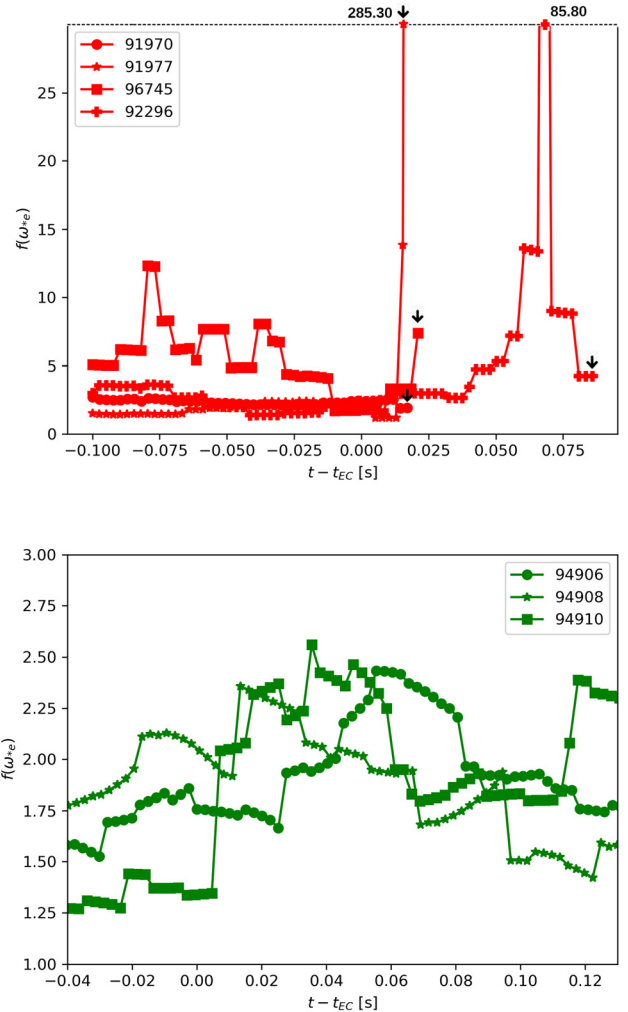


**FIG. 2.** Comparison between the  $f(\omega_{*e})$  vs the time distance from the edge cooling, for the selected pulses. Top: The red traces show the behavior for the unstable pulses. The arrow shows the time of the onset of the mode. Bottom: The green traces represent the behavior of the  $f(\omega_{*e})$  for the stable pulses. It is interesting to highlight that before the onset, we have a peak of the function  $f(\omega_{*e})$ , corresponding to an increment of the destabilizing effect of the ion polarization current, while for the stable pulses  $f(\omega_{*e} \sim 2)$ .



and Sauter. The term<sup>9,12</sup> defined in Eq. (5) represents the destabilizing effect caused by the reduction of the bootstrap current inside the magnetic island. As the island grows, the heat diffusion tends to produce a flattening of the temperature and pressure profiles in the part overlapping the island. The flattening of the pressure reduces the bootstrap current, thus producing a destabilizing effect that boosts the growth of the island.<sup>18</sup> The electron temperature evolves on a fast parallel temperature diffusive equilibration timescale, with a diffusivity  $\chi_{\parallel}$  much larger than  $\chi_{\perp}$ , characterizing the slower perpendicular diffusive transport. In the island region, the balance of the parallel and perpendicular heat flows<sup>16,19</sup> leads to a temperature diffusion equation characterized by a scale length  $W_d \propto (\chi_{\perp}/\chi_{\parallel})^{1/4}$ . The term<sup>9,20</sup>  $\Delta'_{GGJ}$ , defined in Eq. (6), represents the stabilizing term related to the curvature of the plasma inside the torus. This term is modeled heuristically so that it goes as  $1/(kW_d)$  for  $W \ll kW_d$ , avoiding the singularity for  $W \rightarrow 0$ . The constant  $k$  is introduced in order to allow  $\Delta'_{GGJ}$  being greater than  $\Delta'_{boot}$  in the limit of small island. This is important because  $\Delta'_{boot} \sim \sqrt{\varepsilon}$  and  $\Delta'_{GGJ} \sim \varepsilon^2$ , in which the former is intrinsically larger than the latter and the constant  $k$  yields models where the islands become unstable for larger values of width, according to the experiments. The term<sup>9,15,21</sup> in Eq. (7),  $\Delta'_{pol}$ , represents the effect of the IOPC. The magnitude of its contribution depends on the regime of collisionality, according to the function  $g(\omega, \varepsilon, \nu_{ii})$  with  $\nu_{ii} = 4.810^{-8} Z^4 n_i \ln(\Lambda) T_i^{-3/2}$ <sup>22</sup> and  $\ln(\Lambda)$  being the Coulomb logarithm. The formulation, proposed by Mikhailovskii<sup>10</sup> [Eq. (9)], admits three regimes: a low collisionality regime, where the  $\Delta'_{pol}$  is reduced by a factor  $\varepsilon^{3/2}$  due to the reduced interaction between ions flowing outside the island and the plasma, which inhibits the generation IOPC. A mid-collisionality regime followed by a high-collisionality regime where the IOPC is increased by the strong interaction between the ions and the plasma. The limits of the regimes depend on the collisionality ion-ion  $\nu_{ii}$ , the inverse aspect ratio  $\varepsilon$  and the rotation frequency of the island  $\omega$  in the plasma frame of reference. The effect of the ion polarization current can be both stabilizing and destabilizing according to the sign of the function  $f(\omega)$ , shown in Eq. (8) and defined by Smolyakov.<sup>14</sup>  $\omega_{*e}$  and  $\omega_{*i}$  are, respectively, the electron and ion diamagnetic frequencies defined as<sup>23</sup>

$$\omega_{*j} = -\frac{mk_b T_j (dp_j/d\psi)}{e_j p_j q}, \quad (10)$$

with  $j = e, i$ .  $n$  is the poloidal mode number, and  $p'_j$ ,  $e_j$ , and  $n_j$  are, respectively, the radial derivative of the pressure, the charge, and the density of the species  $j$ . The coefficient<sup>21</sup>  $\omega_{*T} = k_{\theta}(dT_i/dr)/(eB_0)$  takes into account the toroidal velocity of the island in the  $f(\omega)$ , connected to the radial derivative of the ion temperature profile  $T_i$  and which is non-negligible at an early stage of development of the island. If  $0 < \omega < \omega_{*i} + \omega_{*T}$ , then  $\Delta'_{pol} < 0$  and its contribution is stabilizing; otherwise, it is destabilizing. Finally, the parameter  $w_{\rho} = O(\rho_{\theta i})$  is introduced in order to let the  $\Delta'_{pol}$  vanish as  $W \ll W_{\rho}$ . This behavior can be explained heuristically by thinking that a current of ions in a magnetized plasma must have at least a width of  $2\rho_i$  so that its contribution to the total longitudinal current of an island with  $W \ll \rho_i$  can be neglected. This is also confirmed by theoretical models developed by Smolyakov,<sup>14</sup> where he investigated the contribution of the ion polarization current in the limit of  $W \ll \rho_i$ , showing that

$$\Delta'_{pol} \sim \frac{1}{W} (\omega - \omega_{*e})(\omega - \omega_{*i}). \quad (11)$$

Other models<sup>24–26</sup> showed that in this limit,  $\omega \rightarrow \omega_{*e}$  so that the overall contribution of the ion polarization current cancels out. An acceptable transition formula from the small to large width limit can be expressed as<sup>9</sup>

$$\Delta'_{pol} \sim \frac{W}{W^4 + W_{\rho}^4}. \quad (12)$$

### III. THE ROLE OF THE LINEAR INDEX $\Delta'_0$

According to the model described in Sec. II A, the stabilizing contribution of the curvature does not vanish when the island width goes to zero. If the  $\Delta'_0$  is positive, then the reconnection of a rational surface is energetically favorable, but this does not imply the onset of an instability. Indeed, the destabilizing strength of the linear term must overcome the stabilizing contribution of the curvature; otherwise, the magnetic island is non-linearly stable. Figure 3 shows the behavior of the non-linear contribution with respect to the island width  $W$ , for an unstable pulse, at the onset of the mode. If the island is smaller than a critical width  $W_{crit}$ , then the stabilizing contribution of the curvature prevents the trigger of the mode. In this picture, a linearly unstable rational surface reconnects, producing a magnetic island with  $W < W_{crit}$ , and then is non-linearly stable and the mode will not grow. The critical width defines how big the reconnection must be in order to produce an instability so that it depends on the linear combination of the linear and non-linear contribution in Eq. (4). The value of  $W_{crit}$  is calculated by computing the smallest zero of the generalized Rutherford equation [Eq. (4)]. In general, the value of the critical width depends also on the strength of the stabilization due to the curvature, the destabilizing contribution of the bootstrap, and the contribution of the ion polarization current. In order to gain a deeper insight about the mechanism that leads to the onset of the mode, the analysis is extended to these terms.

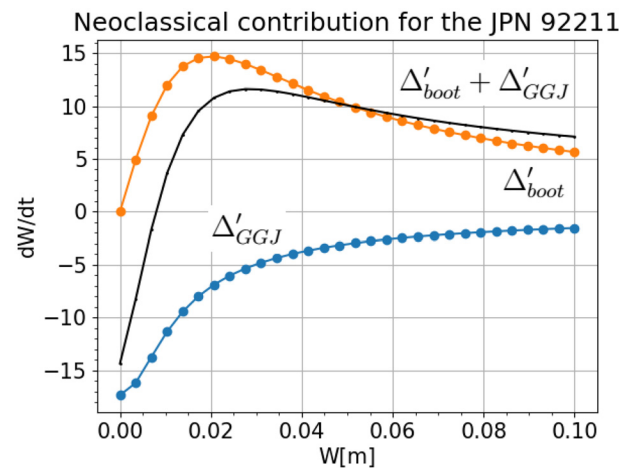


FIG. 3. Illustration showing how the value of  $\Delta'$  changes for the different terms in the generalized Rutherford equation with respect to the island width for a real pulse (JPN 92211) where the coefficients are calculated at the onset of the mode. The orange trace represents  $\Delta'_{boot}$ , the blue trace  $\Delta'_{GGJ}$  adds the black, and their sum  $\Delta'_{boot} + \Delta'_{GGJ}$  goes to zero for small width. There is a region  $W < W_{crit}$  where the sum of the contributions is negative, so an island is stable.

IV. ANALYSIS OF NON-LINEAR TERMS

In this section, a detailed comparison of the competing non-linear terms of the equation governing the growth of magnetic islands is presented, to identify the reason for the onset of the mode in a specific set of JET pulses. The Green–Glasser–Johnson and the bootstrap terms depend on equilibrium quantities (e.g., pressure, safety factor, and current density), so their contributions vary over an equilibrium timescale. On the other hand, the ion polarization current depends on the equilibrium quantities, but its dependence on the island rotation frequency causes the  $\Delta'_{pol}$  to be susceptible to faster fluctuation, which could suddenly change the strength and the sign of the term in the Rutherford’s equation. Although the evolution of the magnetic island is affected by both linear and non-linear phenomena, their effects sum up linearly, so that it is possible to study them separately. First, the analysis is performed by considering only the GGJ and the bootstrap current, and then, it is extended considering also the ion polarization current. The safety factor profile  $q$  and the value of  $\beta$  are taken from an EFIT equilibrium. The electron density and temperature are measured by the interferometer and radiometer diagnostic. The pressure is calculated as the product of the density and the temperature. In the termination phase, data from charge exchange diagnostic are not available because of the lack of neutral beam injection. Ion temperature is estimated from D-D reaction rate in order to evaluate the ions diamagnetic frequency  $\omega_{*i}$ . The ion pressure is calculated from the temperature and the density, assuming  $n_e = n_i$ .

A. Curvature and bootstrap

The analysis is performed over a database composed of 70 disrupting pulses, where the disruption is preceded by the trigger of a magnetic island after an edge cooling. The pulses are classified according to their value of  $q$  on the plasma axis. A reliable indicator of the value of  $q$  on the plasma axis is the sawtooth instability, so its presence implies that  $q_0 < 1$ . Figure 4 shows the position of the database in the plane  $q_{95} - l_i$ . Here,  $l_i$  represents the internal inductance and  $q_{95}$  represents the value of the safety factor  $q$  at the 95% of the minor radius. This allows us to identify the pulses of the database as density limits.<sup>27</sup> The colormap shows that discharges terminating with sawtooth

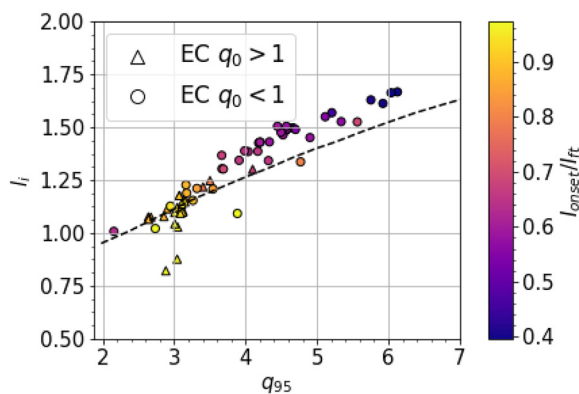


FIG. 4. Position of the pulses of the database in the plane  $l_i - q_{95}$ . The dotted line represents the Wesson density limit. The colorbar shows the ratio between the current at the onset and the current during the pulse. This is a measure of how far the onset happens from the stable plasma operation.

activity ( $q_0 < 1$ ) can be subject to a disruption in the final phase of the current ramp down ( $I_{onset}/I_{ft} < 0.6$ ). As pointed out before, the curvature and the bootstrap terms depend on equilibrium quantities, so, in order to evaluate their effect on the trigger of the mode, it is important to compare, for a certain equilibrium, their respective strength. To do that, the ratio of  $k_{boot} = \beta_p \sqrt{\epsilon} |L_q/L_p|$  to  $k_{GGJ} = \beta_p \epsilon^2 L_q^2 / (r_s |L_p|) \times (1 - 1/q^2)$  is used as a figure of merit. The parameter  $\Theta \equiv k_{GGJ}/k_{boot}$  quantifies how much the coefficient for the stabilizing Green–Glasser–Johnson term is smaller than the destabilizing term of the bootstrap current. A smaller ratio means a more unstable plasma, while a larger ratio means a more stable plasma. It is important to highlight that we are not taking the width of the island into account. A reduction in the ratio does not imply the onset of the mode, but rather a plasma that is more susceptible to the development of instability. The profiles are evaluated at the position of the rational surface, and  $\Theta$  is computed for every pulse at the onset of the mode. Figure 5 shows a histogram of the distribution of the ratio for the pulses in the database. The distribution  $\Theta$  examined during a steady phase of the pulses is larger than the same values tested before the onset of the mode. This is consistent with the physical explanation we provided for the parameter  $\Theta$ : as the parameter decreases, the destabilizing bootstrap term gets larger in comparison with the stabilizing curvature term, increasing the likelihood of the onset of the mode. The two populations of pulses are clearly separated in the figure, showing that for the pulses with  $q_0$  less than 1, the equilibrium configuration corresponds to a lower ratio and more unstable plasma. The magnetic islands are triggered in a more unstable condition, suggesting that the sawtooth contributes to stabilizing the mode. This is consistent with Fig. 4 where the modes in a plasma with  $q_0 < 1$  are triggered later in the termination.

B. Polarization current

The change in the temperature profile due to an edge cooling is found to provide a slight linear destabilization,<sup>1</sup> which is related also to a reduction of the stabilizing contribution of the curvature (GGJ) with respect to the destabilizing bootstrap contribution as shown in Sec. IV A. In the present section, the possible effect of the edge cooling on

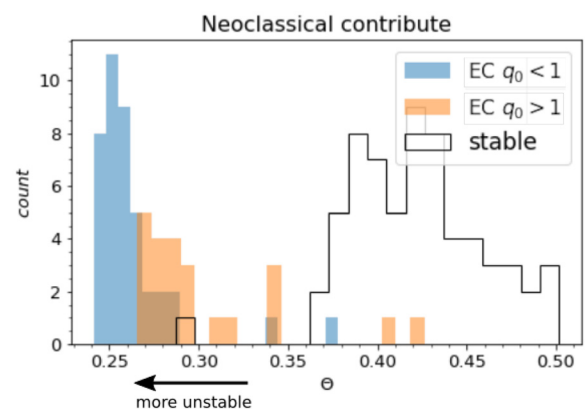
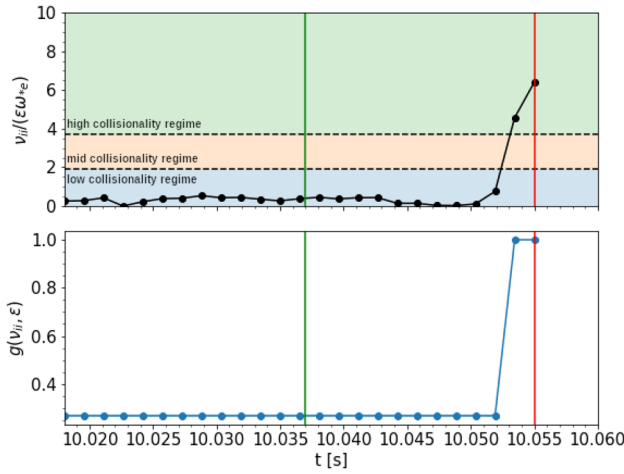


FIG. 5. The distribution of the value of  $\Theta$  for the pulses contained in the database. The blue and orange bars represent pulses with edge cooling, with the value of  $q$  on the axis, respectively, less than 1 and greater than 1. The white bars represent the distribution of  $\Theta$  for the disrupting pulses, calculated during a stable phase of the pulse.



**FIG. 6.** (Top) Time trace of the function  $\nu_{ij}/\epsilon\omega$ . This function determines the value of  $g(\mu_{ij}, \omega)$  (bottom).

the ion polarization current is investigated. The impact of the edge cooling changes the equilibrium profiles, resulting in a contribution of the curvature (GGJ) and bootstrap terms favoring instability. On the other hand, the change in the temperature profile directly modifies the contribution of the IOPC by changing the diamagnetic frequencies contained in the  $f(\omega)$ . In the termination phase, the decrease in the temperature implies an increase in the collisionality, which is taken into account in the generalized Rutherford equation by means of the function  $g(\omega, \epsilon, \nu_{ij})$ , reported in Eq. (4). Figure 6 (bottom) represents the value of the function  $g(\omega, \epsilon, \nu_{ij})$ , close to the onset of the mode, for the pulse 91977. Just before the onset, the collisionality (Fig. 6, top) modifies the value of  $\Delta'_{pol}$ , increasing its contribution. The exact value of the  $\Delta'_{pol}$  depends on the value of the rotation  $\omega$  of the island with respect to the plasma. A measure of the  $\omega$  in the laboratory frame of reference can, in principle, be obtained using the Mirnov coils signals. Then, in order to obtain the rotation frequency with respect to the plasma, we have to subtract the intrinsic  $E \times B$ <sup>8,23,28,29</sup> motion of the plasma, so that

$$\omega = \omega_{Mirnov} - \omega_{E \times B}, \quad (13)$$

$$\omega_{E \times B} = \frac{-n\nu_{\phi j}}{2\pi R} + \frac{n\nabla p_j}{2\pi Z_j n_j R B_\theta}, \quad (14)$$

where  $\nu_{\phi j}$  is the toroidal velocity,  $n$  is the poloidal mode number, and  $\nabla p$ ,  $e_j$ , and  $n_j$  are the radial derivatives of the pressure. The index  $j$  refers to the ion specie that is used as reference for the measure of the toroidal velocity by the charge exchange diagnostic.<sup>8</sup> During the current ramp down, the shutdown of the NBI makes the charge exchange diagnostic not available; therefore, a theoretical approach is needed in order to evaluate the island rotation. According to the theory,<sup>24,30</sup> the island moves in the plasma close to a value, which is the viscosity-weighted mean of the unperturbed electron and ion velocities. Then, it has been shown that, for small island, the island frequency tends to be close to the electron diamagnetic frequency,<sup>25</sup> and this is also confirmed by numerical models.<sup>26</sup> So, the island rotation will be assumed  $\omega = \omega_{*e}$ , and the analysis is focused on the factor  $f(\omega = \omega_{*e})$ . Under this assumption, the nature of the IOPC is always destabilizing for

**TABLE I.** The toroidal magnetic field on the axis, the ratio between the current at the onset of the mode and the current at the flat top, and the value of the poloidal ionic Larmor radius are reported to allow a comparison between the pulses. Furthermore, we reported the first measured width.

Pulse	$B_t$ (T)	$I_{onset}/I_{ft}$	$\rho_{0i}$ (cm)	$\min(w_{measured})$ (cm)
91977	2.69	0.95	0.88	2.92
92296	2.78	0.90	1.10	5.76
96745	2.77	0.95	0.73	4.72
91970	2.71	0.89	0.95	2.10

small island. This is consistent with some recent theoretical works.<sup>31</sup> The diamagnetic frequencies are calculated using the ionic and electronic pressure profiles measured by the diagnostics. In the majority of the pulses in the database, the ion temperature is assumed to be equal to the electron temperature. Generally speaking, this is a reasonable approximation while the species are at equilibrium, but during the termination phase, it may be a rough approximation that hides the differences between the diamagnetic frequencies. For this reason, the pulses of the database are filtered in order to neglect the pulses where  $T_e = T_i$ . From the starting database, we selected four disrupting pulses. Table I reports the characteristic quantities of the selected pulses. In particular, it is noteworthy that the resolution of the Mirnov coils allows us to detect the island only when the island  $W$  is larger than the ion Larmor radius  $\rho_{0i}$  so that the Mirnov measures cannot be exploited to estimate the island rotation frequency at the very beginning of the island evolution. Along with these, we also selected three pulses, which develop an edge cooling without developing a tearing mode. In order to provide a complete physical picture of the pulses that we analyzed, we present here a description of the behavior of the pulse 91977. The plasma current is 3 mA, and the toroidal magnetic field is 2.69 T. At the beginning of the ramp down of the current ( $I_{onset}/I_{flat-top} \simeq 0.95$ ), the pulse experiences an edge cooling, which starts at 10.037 s. The onset of the mode occurs at 10.055 s. The spectrogram of the Mirnov coils signals (Fig. 7) shows the magnetic perturbation caused by the 2/1 mode and the 1/1 mode (connected to the sawtooth crashes). Figure 8 shows the evolution of the island evaluated using the magnetic perturbation measured by the magnetic coils, according to<sup>32</sup>

$$W = 4 \sqrt{\frac{R_0 r_s}{n B_T s_s} \frac{1}{2} \left( \frac{r_c}{r_s} \right)^{m+1} \tilde{B}_\theta}, \quad (15)$$

where  $n$  is the toroidal mode number;  $B_T$ ,  $r_s$ ,  $R_0$ , and  $s_s$  are the toroidal magnetic field, the position of the rational surface, the major radius, and the magnetic shear evaluated by the EFIT equilibrium, respectively.  $\tilde{B}_\theta$  is the poloidal perturbed magnetic field. The expression (15) is valid for modes with  $m \geq 2$  and under the assumption that the position of the coils  $r_c$  coincides with that of the wall. The first measure of the amplitude of the magnetic field perturbation provides an island width of 2.92 cm. During its growth, the mode slows down, as it is evident by the reduction of the frequency in the spectrogram, which is reported in Fig. 8 (gray line). The mode grows till 30 cm, when locks at 10.064 s and disrupts the plasma at 10.112 s. Figure 2 represents the time traces of the factor  $f(\omega_{*e})$  for the selected pulses. The behavior of  $f(\omega_{*e})$  is similar for the safe pulses. In particular, we have  $f(\omega_{*e}) \simeq 2$ , meaning that  $|\omega_{*e}| \simeq |\omega_{*i}|$ . This represents the thermal equilibrium

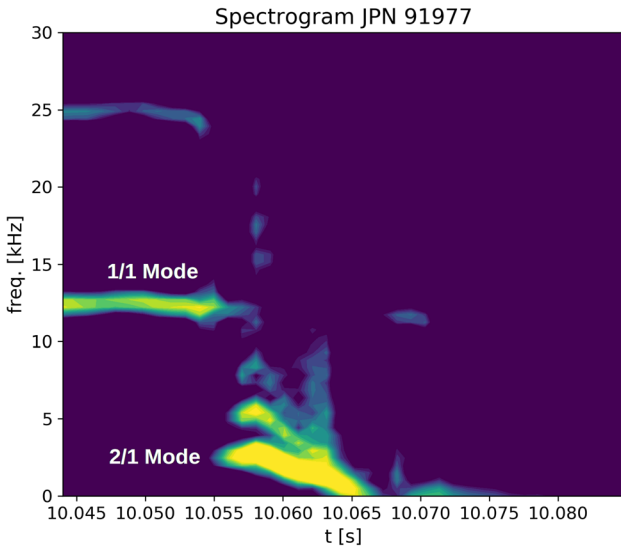


**FIG. 7.** Frequency spectrogram of the signal of the Mirnov coils vs time. The 2/1 mode can be seen starting from  $t \simeq 10.05$  s, when it slows down till the locking at  $t \simeq 10.064$ . It is also possible to distinguish the magnetic activity of the 1/1 mode, connected to the sawtooth crashes.

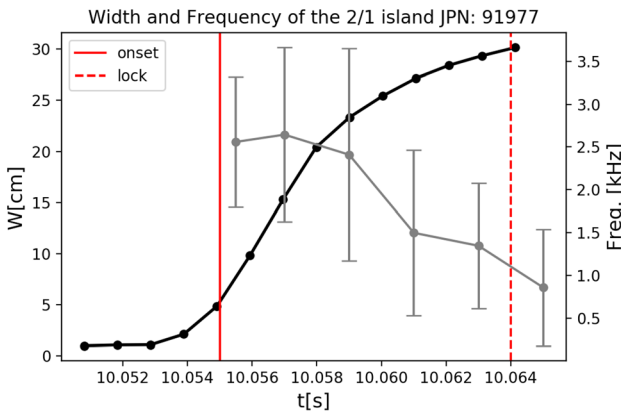


**FIG. 8.** The evolution of the island width (black line) for the disrupting pulse 91977. The mode starts at 10.055 s leading to disruption. The gray line represents the rotation frequency of the mode measured by the Mirnov coils.

value when  $T_e \simeq T_i$ . In the unstable pulses, the function  $f(\omega_{*e})$  shows strong increment of the function before the onset. The peak of the function  $f(\omega_{*e})$  corresponds to a stronger destabilizing effect of the IOPC at that time. The pulse 91970 is the only one that does not follow this behavior: the value of  $f(\omega_{*e})$  oscillates, and there is no particular increment between the edge cooling and the onset of the mode. The values of  $f(\omega_{*e})$  at the onset are higher with respect to the equilibrium value for three pulses out of four. The reason why the parameter  $f(\omega_{*e})$  is so high is the reduction of the electron diamagnetic frequency compared to the ion diamagnetic frequency as a consequence of the edge cooling. The results suggest that the effect of the edge

cooling is to increase the destabilizing effect of the ion polarization current. It is important to highlight that any kind of fluctuations of the temperature profile could correspond to a fluctuation of the IOPC, which could pass very quickly from stabilizing to destabilizing. In general, this analysis suggests that the ion polarization current represents a key contribution, which leads to a more unstable configuration and suddenly increases the probability of onset of the mode.

**V. CRITICAL WIDTH**

The theory of the (neoclassical) tearing mode introduces the idea of critical width: given a seed island of width  $W_{seed}$ , the  $W_{crit}$  is that width such that if  $W_{seed} > W_{crit}$ , then the seed island becomes unstable.  $W_{crit}$  can be seen as an indicator of the stability condition of the plasma because the smaller the critical width, the simpler it is for a perturbation to cause an instability. The critical width is calculated as the zero of the generalized Rutherford equation, evaluated by summing the contributions of the curvature ( $\Delta'_{GG}$ ), the bootstrap ( $\Delta'_{boot}$ ), the ion polarization current ( $\Delta'_{pol}$ ), and the linear contribution ( $\Delta'_0$ ). For a given time  $t$ , the critical width  $W_{crit}(t)$  is calculated by evaluating the  $dW/dt$  for every width and taking the width such that  $dW/dt = 0$ .

In order to highlight the effect of the ion polarization current on the critical width, Fig. 9 shows the value of the critical width vs time, for a real pulse, considering and neglecting the ion polarization current. The effect of the ion polarization current is to reduce the critical width just before the onset of the mode. Figure 10 shows the trace of every single contribution for a fixed width ( $W = 0.005 \sim W_{crit}$  in this case). The sign of the sum (black line) determines if the mode is stable or unstable. If the sum is positive, then the mode is unstable, otherwise is stable. The linear contribution  $\Delta'_0$  can be calculated using the equilibrium current density profile. However, the time resolution needed in this phase of the pulse is high, so the data are not resolved enough to follow the evolution of the mode in the edge cooling timescale. In order to highlight the contribution of the non-linear terms, the plasma is taken to be linearly stable so that  $r_s \Delta'_0 = -m$ . The trigger of the mode is determined by an increase in the destabilizing effect of the IOPC and a decrease in the stabilizing curvature effect with respect to the bootstrap current. The island rotation is fixed to be equal to the electron diamagnetic frequency, as we are focusing in the first phase of the evolution of the mode; therefore, the island can be considered in

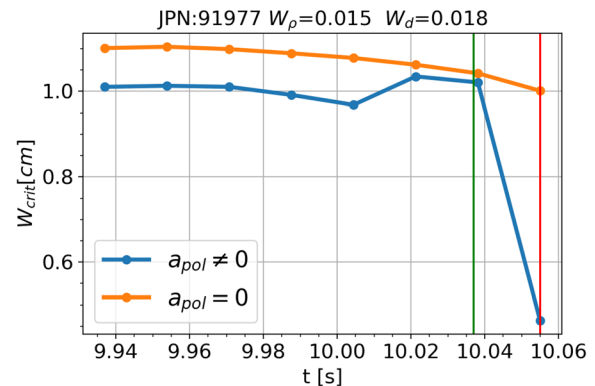


**FIG. 9.** The time trace of the critical width of the pulse 91977, taking in to consideration the effect of the ion polarization current (blue trace) and neglecting it (orange trace).

25 October 2024 17:42:10



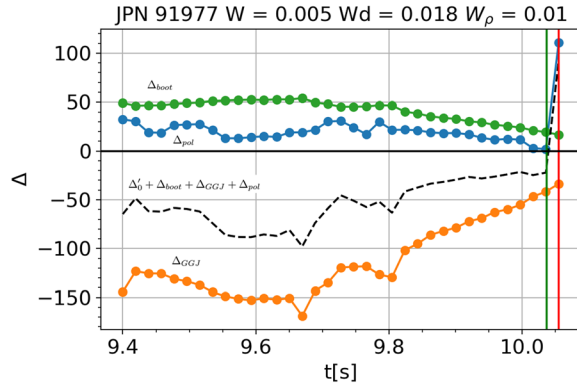


**FIG. 10.** The time trace of the contributions of the generalized Rutherford equation for the 91977. The vertical green and red lines represent, respectively, the time of the edge cooling and the time of the onset of the mode.

the small width limit described in Sec. IV B. The ion polarization current dominates the curve for small  $W$  ( $W_\rho \sim W < W_d$ ) and its effect is to reduce the  $W_{crit}$  from  $W_{crit}(a_{pol} = 0) = 1.01\text{cm}$  to  $W_{crit}(a_{pol} \neq 0) = 0.47\text{cm}$ . The same analysis is carried out over the selected pulses, and the results are summarized in Table II.

The reduction of the critical width is more evident for higher values of  $f(\omega_{*e})$ , while it is small for the 91970, where the destabilizing contribution of the ion polarization current is weaker. The analysis is performed over a restricted subset of pulses due to lack of data, but some general behavior can be inferred. The model shows that for fluctuations of the ion polarization current, a consequence of the flattening of the temperature profile due to the edge cooling is that the value of the  $W_{crit}$  decreases, leading to a more unstable condition for the 2/1 rational surface. The effect of the fluctuation of the IOPC is higher when the flattening due to the EC gets closer to the rational surface, as  $\Delta'_{pol}$  depends on local quantities, such as the rotation and the collisionality. This can be verified for the other pulses, despite the lack of data in the termination phase. Defining a threshold  $\kappa$  and a flattening width such as

$$r_{flattening} = \min \left( r \in (0, 1) \text{ s.t. } \left| \frac{dT_e}{dr} \right| < \kappa \right), \quad (16)$$

we can infer an onset criteria based on the fluctuation of the ion polarization current from that analysis. Figure 11 shows the position of the rational surface (red line) and the width of the flattening (black lines) as defined in Eq. (16) at the onset of the mode, for the pulse 91977. In particular, it has been shown that a flattening of the temperature

**TABLE II.** Summary of the critical width, calculated with and without the contribution of the ion polarization current.

Pulse	$w_{crit}(a_{pol} = 0)$ (cm)	$w_{crit}(a_{po} \neq 0)$ (cm)
91977	1.01	0.47
92296	1.18	0.60
96745	1.00	0.35
91970	0.99	0.89

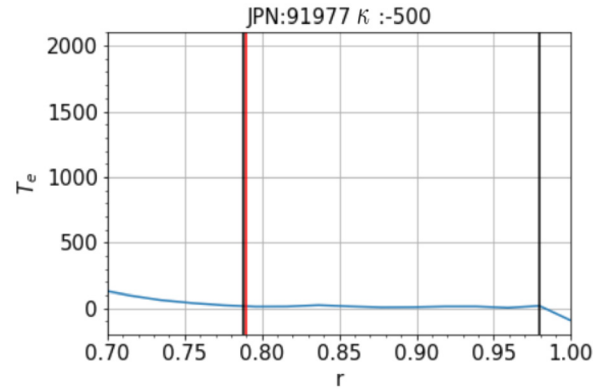


**FIG. 11.** Example of the algorithm used to calculate the position of the flattening compared to the position of the rational surface. Here, the temperature profile at the onset of the mode for the pulse 91977 is shown. The black vertical lines show the flattening width. The red vertical line represents the position of the rational surface.

profile reduces the value of the electron diamagnetic frequency, increasing the destabilizing contribution of the  $\Delta'_{pol}$ . This happens when the flattening of the rational surface causes a consistent fluctuation of the temperature, namely, when  $r_s > \gamma r_{flattening}$ . Here,  $\gamma \sim O(1)$  is a constant that takes into account that the flattening does not necessarily have to reach the rational surface for the temperature fluctuation to be strong enough to modify the contribution of the ion polarization current and then trigger the mode.

Figure 12 shows the position in this plane for the pulses contained in the database. The dashed black line represents  $r_s = r_{flattening}$ , so, according to the interpretation given by this model, we can see that the most of the pulses stay in the region  $r_s > r_{flattening}$ . The threshold obtained for  $\gamma = 0.81$  splits the plane in two parts, such that every

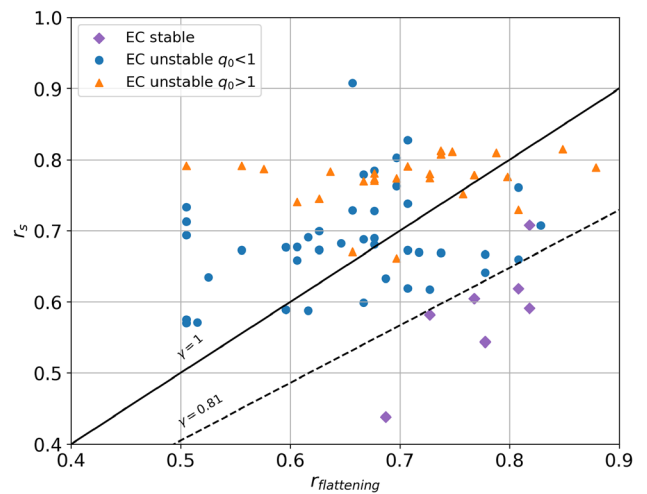


**FIG. 12.** Position in the plane  $(r_{flattening}, r_s)$  of the edge cooling pulses of the database. The purple dots represent the edge cooling that does not trigger a mode. The blue and orange dots represents, respectively, the edge cooling with  $q_0 < 1$  and  $q_0 > 1$ . The position is calculated at the onset of the mode for the disrupting pulses and by taking the temperature profile with the wider flattening within 200 ms (median time of onset according to Ref. 1) after the edge cooling for the purple dots.

analyzed pulses overcomes the threshold and then develops a neoclassical tearing mode. The stable pulses (purple dots) do not overcome the threshold except for one pulse that slightly exceeds the dashed line. Figure 12 shows that, in these cases, the flattening of the temperature profile does not reach the position of the resonant surface, reducing the fluctuation of the ion polarization contribution and, according to the analysis, preventing the onset of the mode.

## VI. CONCLUSION

The stability of a tokamak equilibrium with respect to the tearing perturbations depends on the linear stability index  $\Delta'_0$  and the non-linear terms (the curvature and the bootstrap term) in the Rutherford equation. The equilibrium configuration determines the trigger of the mode affecting the  $\Delta'_0$ ,  $\Delta_{GGJ}$ , and  $\Delta_{boot}$ . As shown in Sec. III, the linear stability index does not completely describe the mechanism of triggering a mode because the stabilizing effect of the curvature could prevent the onset of the mode also for positive value of  $\Delta'_0$ . It is more suitable to think in terms of the critical width, which can be seen as a quantity proportional to the likelihood of triggering a mode. In this picture, the role of the  $\Delta'_0$  is to reduce the value of the critical width to increase the probability of onset of a mode. On the equilibrium timescale, the value of the critical width is represented by a balance between the Green–Glasser–Johnson term, the bootstrap term, and the linear term. However, the value of the critical width can be affected also by faster fluctuations, which change the rotation frequency of the island, leading to a more unstable plasma due to the ion polarization current. Here, a database of disrupting pulses is considered. The analysis of the neoclassical phenomena (GGJ and bootstrap), in Sec. IV A, pointed out that, for the analyzed pulses, the ratio  $\Theta \equiv k_{GGJ}/k_{boot}$  is lower at the onset of the mode than during a stable phase (Fig. 5). This is consistent because it corresponds to a decrease in the stabilizing effect of the curvature with respect to the destabilizing effect of the bootstrap current, thus raising the probability of triggering a mode. Then, the analysis performed over a subset of selected pulses in Sec. IV B highlights that fluctuations of the temperature profiles, in consequence of the edge cooling, lead to an increase in the destabilizing effect of the IOPC by increasing the value of  $f(\omega)$ . The interpretation proposed for a small subset of pulses has been generalized and used to predict a general behavior for every pulse of the database, which is consistent with the results. In fact, it has been shown in Fig. 12 that, after an edge cooling, a pulse tends to develop a mode whenever the flattening, as a consequence of the edge cooling, reaches the position of the rational surface. At this point, the function  $f(\omega)$  increases due to the reduction of the electron diamagnetic frequency, confirming that the ion polarization current has a key role in the onset of the mode. The analysis has been carried out by treating every single contribution of Eq. (4) separately. This can be done due to the form of the model we are using: the effect of every contribution, though non-linear, sums up linearly. Even though the validity of these results is restricted to a specific case of onset (i.e., in termination phase, after an edge cooling), the analysis suggests a new general explanation for the trigger of the mode. A noisy fluctuation of the  $f(\omega)$  could lead to a reduction of the critical width at some time. This corresponds to a condition where it is more likely for a random resonant helical perturbation to produce a seed island larger than the critical width, leading to an instability. The IOPC introduces randomness<sup>33</sup> in the problem of the onset of the mode, such that it is more suitable to define the stability using a probabilistic approach.

## ACKNOWLEDGMENTS

This work has been carried out within the framework of the EUROfusion Consortium, funded by the European Union via the Euratom Research and Training Programme (Grant Agreement No. 101052200 EUROfusion). Views and opinions expressed are, however, those of the author(s) only and do not necessarily reflect those of the European Union or the European Commission. Neither the European Union nor the European Commission can be held responsible for them.

## AUTHOR DECLARATIONS

### Conflict of Interest

The authors have no conflicts to disclose.

### Author Contributions

**L. Bonalumi:** Conceptualization (lead); Data curation (lead); Formal analysis (lead); Investigation (lead); Methodology (lead); Software (lead); Validation (lead); Visualization (lead); Writing – original draft (lead); Writing – review & editing (lead). **E. Alessi:** Conceptualization (equal); Investigation (equal); Supervision (equal); Writing – review & editing (equal). **E. Lazzaro:** Conceptualization (equal); Methodology (equal); Supervision (equal); Writing – review & editing (equal). **S. Nowak:** Conceptualization (equal); Investigation (equal); Supervision (equal); Writing – review & editing (equal). **C. Sozzi:** Project administration (equal); Supervision (equal); Writing – review & editing (equal). **D. Frigione:** Data curation (equal). **L. Garzotti:** Data curation (equal). **E. Lerche:** Data curation (equal). **F. Rimini:** Data curation (equal). **D. Van Eester:** Data curation (equal).

## DATA AVAILABILITY

The data that support the findings of this study are available from JET-Eurofusion. Restrictions apply to the availability of these data, which were used under license for this study. Data are available from the authors upon reasonable request and with the permission of JET-Eurofusion.

## REFERENCES

- <sup>1</sup>G. Pucella, P. Buratti, E. Giovannozzi, E. Alessi, F. Auriemma, D. Brunetti, D. R. Ferreira, M. Baruzzo, D. Frigione, L. Garzotti *et al.*, “Onset of tearing modes in plasma termination on jet: The role of temperature hollowing and edge cooling,” *Nucl. Fusion* **61**, 046020 (2021).
- <sup>2</sup>C. Sozzi, E. Alessi, P. J. Lomas, F. Rimini, C. Stuart, C. Challis, L. Garzotti, M. Lemmholm, S. Gerasinov, C. Maggi *et al.*, “Termination of discharges in high performance scenarios in jet,” in *Poster Presented at 28th IAEA Fusion Energy Conference (FEC, 2020)*, pp. 1–7.
- <sup>3</sup>P. C. D. Vries, M. F. Johnson, B. Alper, P. Buratti, T. C. Hender, H. R. Koslowski, and V. Riccardo, “Survey of disruption causes at JET,” *Nucl. Fusion* **51**, 053018 (2011).
- <sup>4</sup>P. H. Rutherford, “Nonlinear growth of the tearing mode,” *Phys. Fluids* **16**, 1903–1908 (1973).
- <sup>5</sup>P. Rebut and M. Hugon, “Magnetic turbulence self-sustainment by finite larmor radius effect,” *Plasma Phys. Controlled Fusion* **33**, 1085 (1991).
- <sup>6</sup>X. Garbet, F. Mourgues, and A. Samain, “Non-linear self consistency of micro-tearing modes,” *Plasma Phys. Controlled Fusion* **30**, 343 (1988).
- <sup>7</sup>E. Poli, A. Bergmann, A. G. Peeters, L. C. Appel, and S. D. Pinches, “Kinetic calculation of the polarization current in the presence of a neoclassical tearing mode,” *Nucl. Fusion* **45**, 384 (2005).

- <sup>8</sup>R. J. L. Haye, C. C. Petty, E. J. Strait, F. L. Waelbroeck, and H. R. Wilson, "Propagation of magnetic islands in the  $E_r=0$  frame of co-injected neutral beam driven discharges in the diii-d tokamak," *Phys. Plasmas* **10**, 3644–3648 (2003).
- <sup>9</sup>E. Lazzaro, D. Borgogno, D. Brunetti, L. Comisso, O. Fevrier, D. Grasso, H. Lutjens, P. Maget, S. Nowak, O. Sauter, and C. Sozzi, "Physics conditions for robust control of tearing modes in a rotating tokamak plasma," *Plasma Phys. Controlled Fusion* **60**, 014044 (2018).
- <sup>10</sup>A. B. Mikhailovskii, "Theory of magnetic islands in tokamaks with accenting neoclassical tearing modes," *Contrib. Plasma Phys.* **43**, 125–177 (2003).
- <sup>11</sup>A. V. Dudkovskaia, J. W. Connor, D. Dickinson, P. Hill, K. Imada, S. Leigh, and H. R. Wilson, "Drift kinetic theory of neoclassical tearing modes in a low collisionality tokamak plasma: Magnetic island threshold physics," *Plasma Phys. Controlled Fusion* **63**, 054001 (2021).
- <sup>12</sup>C. C. Hegna and J. D. Callen, "Interaction of bootstrap-current-driven magnetic islands," *Phys. Fluids B* **4**, 1855–1866 (1992).
- <sup>13</sup>V. Basiuk, P. Huynh, A. Merle, S. Nowak, O. Sauter, J. Contributors, E.-I. Team *et al.*, "Towards self-consistent plasma modelisation in presence of neoclassical tearing mode and sawteeth: Effects on transport coefficients," *Plasma Phys. Controlled Fusion* **59**, 125012 (2017).
- <sup>14</sup>A. I. Smolyakov, "Nonlinear evolution of tearing modes in inhomogeneous plasmas," *Plasma Phys. Controlled Fusion* **35**, 657 (1993).
- <sup>15</sup>A. Smolyakov, "Drift magnetic islands in a tokamak," *Fizika Plazmy* **15**, 1153–1159 (1989).
- <sup>16</sup>O. Sauter, R. Buttery, R. Felton, T. Hender, D. Howell *et al.*, "Marginal  $\beta$ -limit for neoclassical tearing modes in jet H-mode discharges," *Plasma Phys. Controlled Fusion* **44**, 1999 (2002).
- <sup>17</sup>H. Zohm, "Stabilization of neoclassical tearing modes by electron cyclotron current drive," *Phys. Plasmas* **4**, 3433–3435 (1997).
- <sup>18</sup>O. Sauter, R. J. L. Haye, Z. Chang, D. A. Gates, Y. Kamada, H. Zohm, A. Bondeson, D. Bouchers, J. D. Callen, M. S. Chu *et al.*, "Beta limits in long-pulse tokamak discharges," *Phys. Plasmas* **4**, 1654–1664 (1997).
- <sup>19</sup>R. Fitzpatrick, "Helical temperature perturbations associated with tearing modes in tokamak plasmas," *Phys. Plasmas* **2**, 825–838 (1995).
- <sup>20</sup>A. Glasser, J. M. Greene, and J. Johnson, "Resistive instabilities in a tokamak," *Phys. Fluids* **19**, 567–574 (1976).
- <sup>21</sup>A. I. Smolyakov, A. Hirose, E. Lazzaro, G. B. Re, and J. D. Callen, "Rotating nonlinear magnetic islands in a tokamak plasma," *Phys. Plasmas* **2**, 1581–1598 (1995).
- <sup>22</sup>D. L. Book, *NRL (Naval Research Laboratory) Plasma Formulary, Revised* (DTIC, 2007).
- <sup>23</sup>P. Buratti, E. Alessi, M. Baruzzo, A. Casolari, E. Giovannozzi, C. Giroud, N. Hawkes, S. Menmuir, and G. Pucella, "Diagnostic application of magnetic islands rotation in jet," *Nucl. Fusion* **56**, 076004 (2016).
- <sup>24</sup>R. Fitzpatrick and F. L. Waelbroeck, "Two-fluid magnetic island dynamics in slab geometry. I. Isolated islands," *Phys. Plasmas* **12**, 022307 (2005).
- <sup>25</sup>R. Fitzpatrick and F. L. Waelbroeck, "Drift-tearing magnetic islands in tokamak plasmas," *Phys. Plasmas* **15**, 012502 (2008).
- <sup>26</sup>A. Ishizawa, F. L. Waelbroeck, R. Fitzpatrick, W. Horton, and N. Nakajima, "Magnetic island evolution in hot ion plasmas," *Phys. Plasmas* **19**, 072312 (2012).
- <sup>27</sup>J. Snipes, D. Campbell, P. Haynes, T. Hender, M. Hugon, P. Lomas, N. L. Cardozo, M. Nave, and F. Schüller, "Large amplitude quasi-stationary MHD modes in jet," *Nucl. Fusion* **28**, 1085 (1988).
- <sup>28</sup>F. L. Hinten and J. A. Robertson, "Neoclassical dielectric property of a tokamak plasma," *Phys. Fluids* **27**, 1243–1247 (1984).
- <sup>29</sup>T. Ozeki, A. Smolyakov, A. Isayama, N. Takei, N. Hayashi, and S. Takeji, "Effects of plasma rotation on the neoclassical tearing mode in JT-60U," *Plasma Fusion Res.* **5**, 037 (2001).
- <sup>30</sup>F. L. Waelbroeck, "Natural velocity of magnetic islands," *Phys. Rev. Lett.* **95**, 035002 (2005).
- <sup>31</sup>A. Dudkovskaia, J. Connor, D. Dickinson, P. Hill, K. Imada, S. Leigh, and H. R. Wilson, "Drift kinetic theory of neoclassical tearing modes in tokamak plasmas: Polarisation current and its effect on magnetic island threshold physics," *Nucl. Fusion* **63**, 126040 (2023).
- <sup>32</sup>G. Pucella, E. Alessi, F. Auriemma, P. Buratti, M. V. Falessi, E. Giovannozzi, F. Zonca, M. Baruzzo, C. D. Challis, R. Dumont, D. Frigione, L. Garzotti, J. Hobirk, A. Kappatou, D. L. Keeling, D. King, V. G. Kiptily, E. Lerche, P. J. Lomas, M. Maslov, I. Nunes, F. Rimini, P. Sirén, C. Sozzi, M. F. Stamp, Z. Stancar, H. Sun, D. V. Eester, M. Zerbini, and J. Contributors, "Beta-induced Alfvén eigenmodes and geodesic acoustic modes in the presence of strong tearing activity during the current ramp-down on jet," *Plasma Phys. Controlled Fusion* **64**, 045023 (2022).
- <sup>33</sup>L. Bardoczi, N. Richner, and N. Logan, "The onset distribution of rotating tearing modes and its consequences on the stability of high-confinement-mode plasmas in DIII-D," *Nucl. Fusion* **63**, 126052 (2023).